Development of *N*-Alkyl-Substituted Bis(pyrrolo[3,4-*d*])tetrathiafulvalenes as Organic Semiconductors for Solution-Processible Field-Effect Transistors

Iori Doi,[†] Eigo Miyazaki,[†] Kazuo Takimiya,*[,†,‡] and Yoshihito Kunugi[§]

Department of Applied Chemistry, Graduate School of Engineering, Hiroshima University, Higashi-Hiroshima 739-8527, Japan, Institute for Advanced Materials Research, Hiroshima University, Higashi-Hiroshima 739-8530, Japan, and Department of Applied Chemistry, Faculty of Engineering, Tokai University, 1117 Kitakaname, Hiratsuka 259-1292, Japan

Received April 6, 2007. Revised Manuscript Received August 4, 2007

A series of *N*-alkyl-substituted bis(pyrrolo[3,4-*d*])tetrathiafulvalenes (PyTTFs, alkyl = *n*-butyl, *n*-octyl, *n*-dodecyl, *n*-cetyl, and *n*-icosyl, **3**−**7**) were synthesized as highly soluble tetrathiafulvalene (TTF) derivatives. Their solid-state structures were characterized by X-ray diffraction, and their suitability for use as semiconductors for solution-processible organic field-effect transistor (OFET) devices was evaluated. Whereas the solubility of the TTF derivatives was enhanced with the introduction of alkyl groups, very long alkyl groups, such as the *n*-icosyl group, reduced the solubility probably due to intermolecular hydrophobic interactions between the very long alkyl groups. The solid-state structure was also influenced by the length of the alkyl groups; molecules **5**−**7** having *n*-dodecyl or longer alkyl groups tended to assume two-dimensional (2-D) molecular ordering both in the bulk single crystals and in the spin-coated thin films. In contrast, **3** and **4**, having short *n*-butyl and *n*-octyl groups, did not take on a 2-D interactive structure in the solid state. Consistent with the solid-state structure of the PyTTF derivatives, field-effect transistor (FET) characteristics of the solution-processed OFETs markedly depended on the length of the alkyl groups. In contrast to spin-coated thin films of **3** and **4**, which were relatively inferior semiconducting layers ($\mu_{FET} = \sim 10^{-5}$ cm^2 V^{-1} s^{-1} or no reproducible field effect), OFET devices consisting of spin-coated thin films of **5**−**7** showed typical *p*-channel FET characteristics, namely, hole mobilities of $\sim 10^{-2}$ cm^2 V^{-1} s^{-1} and current on/off ratios of $\sim 10^4$. The results indicate that an appropriate combination of a π-conjugated core with long alkyl groups could provide soluble organic semiconductors that are applicable to solution-processible OFETs.

Introduction

Soluble organic semiconductors have been attracting interest due to their low cost and utility in the large-area fabrication of organic thin-film-based electronic devices such as organic light-emitting diodes (OLEDs) and organic field-effect transistors (OFETs).[1,2] Conjugated polymers and oligomers (e.g., polythiophenes,[3] thiophene-containing copolymers,[4] oligothiophenes,[5] and soluble precursors of pentacene)[6] have been employed as active semiconducting layers for solution-processible OFETs. Despite the good device performance attained by recently developed thienothiophene-containing copolymers[4b] [field-effect mobility (μ_{FET}) = ∼0.7 cm^2 V^{-1} s^{-1} and current on/off ratio (I_{on}/I_{off}) = $\sim 10^6$], which is comparable to that of the best vapor-deposited OFETs, generally speaking, the performance in terms of μ_{FET} and I_{on}/I_{off} of solution-processible OFETs is lower than that of vapor-deposited ones.

As another approach to developing soluble organic semiconductors, several research groups have focused on small π-conjugated molecules with solubilizing substituents.[7,8] Recently, the production of superior solution-processible OFETs with $\mu_{FET} = \sim 1.0$ cm^2 V^{-1} s^{-1} using soluble anthradithiophene-based devices has been reported.[9] As opposed to large-polymer-based materials, the advantages of using these small molecules include the ease of purification and the ability to precisely control their molecular structures and properties, such as solubility, ionization

* Corresponding author. E-mail: ktakimi@hiroshima-u.ac.jp.
† Graduate School of Engineering, Hiroshima University.
‡ Institute for Advanced Materials Research, Hiroshima University.
§ Tokai University.

(1) Recently, a special issue on organic electronics was published: Jenekhe, S. A. *Chem. Mater.* **2004**, *16*, 4381−4846.
(2) (a) Dimitrakopoulos, C. D.; Malenfant, P. R. L. *Adv. Mater.* **2002**, *14*, 99−117. (b) Katz, H. E. *Chem. Mater.* **2004**, *16*, 4748−4756. (c) Sirringhaus, H. *Adv. Mater.* **2005**, *17*, 2411−2425.
(3) (a) Bao, Z.; Dodabalapur, A.; Lovinger, A. J. *Appl. Phys. Lett.* **1996**, *69*, 4108−4110. (b) Sirringhaus, H.; Tessler, N.; Friend, R. H. *Science* **1998**, *280*, 1741−1744. (c) Sirringhaus, H.; Brown, P. J.; Friend, R. H.; Nielsen, M. M.; Bechgaard, K.; Langeveld-Voss, B. M. W.; Spiering, A. J. H.; Janssen, R. A. J.; Meijer, E. W.; Herwig, P.; de Leeuw, D. M. *Nature* **1999**, *401*, 685−688. (d) Wang, G. M.; Swensen, J.; Moses, D.; Heeger, A. J. *J. Appl. Phys.* **2003**, *93*, 6137−6141. (e) Chang, J.-F.; Sun, B.; Breiby, D. W.; Nielsen, M. M.; Sölling, T. I.; Giles, M.; McCulloch, I.; Sirringhaus, H. *Chem. Mater.* **2004**, *16*, 4772−4776. (f) Kline, R. J.; McGehee, M. D.; Kadnikova, E. N.; Liu, J.; Fréchet, J. M. J. *Adv. Mater.* **2003**, *15*, 1519−1522. (g) Kline, R. J.; McGehee, M. D.; Toney, M. F. *Nat. Mater.* **2006**, *5*, 222−228. (h) Ong, B. S.; Wu, Y.; Liu, P.; Gardner, S. *J. Am. Chem. Soc.* **2004**, *126*, 3378−3379. (i) Wu, Y.; Liu, P.; Gardner, S.; Ong, B. S. *Chem. Mater.* **2005**, *17*, 221−223. (j) Ong, B. S.; Wu, Y.; Liu, P.; Gardner, S. *Adv. Mater.* **2005**, *17*, 1141−1144. (k) Liu, P.; Wu, Y.; Li, Y.; Ong, B. S.; Zhu, S. *J. Am. Chem. Soc.* **2006**, *128*, 4554−4555. (l) Murphy, A. R.; Liu, J.; Luscombe, C.; Kavulak, D.; Fréchet, J. M. J.; Kline, R. J.; McGehee, M. D. *Chem. Mater.* **2005**, *17*, 4892−4899.

10.1021/cm070956+ CCC: $37.00
Published on Web 09/29/2007

potential (IP), and HOMO−LUMO gap. However, even subtle structural modifications of these small molecules can change the molecular ordering in the thin-film state, resulting in drastic effects on the performance of the FET.[9] In other words, the difficulty of developing soluble organic semiconductors based on small π-conjugated molecules lies in balancing the cohesive nature of the π-core with the steric bulkiness of the attached solubilizing groups, the latter deterring effective overlapping between π-cores in the thin-film state.[9]

Tetrathiafulvalene (TTF) has a small π-core and possesses a high self-aggregation ability due to its four sulfur atoms. It is well-known as a representative electron donor skeleton for molecular conductors and superconductors.[10] With interest in OFETs increasing at a rapid pace, TTF derivatives have been examined as active semiconducting materials.[11,12] Using aromatic-ring-fused TTF derivatives such as benzene, thiophene, naphthalene, pyridine, and related nitrogen-containing aromatic moieties, impressive FET characteristics, both in single-crystal-based devices ($\mu_{FET} = \sim 1.4$ cm^2 V^{-1} s^{-1}) and in thin-film-based devices ($\mu_{FET} = \sim 0.6$ cm^2 V^{-1} s^{-1}), have been reported.[13]

Considering the benefits of the strong cohesive character of the TTF cores, we have identified TTF as a promising π-conjugated core for use as a soluble conducting material in OFETs.[14] It may be designed to include two long aliphatic chains in such a way that the resulting molecules can assume a stretched structure along the TTF long-axis direction, where the introduced aliphatic chains will not hinder intermolecular $\pi-\pi$ and/or transverse sulfur−sulfur interactions. However, when disubstitution on each 1,3-dithiole ring is carried out, cis/trans isomerization of the central double bond in the TTF core readily occurs. This results in the formation of a mixture of two isomers having very different molecular shapes[12,15] that are not optimal for the formation of highly ordered molecular arrays in the thin-film state. Therefore, as the bis(pyrrolo[3,4-*d*])tetrathiafulvalene (PyTTF) structure with two *N*-alkyl groups contains no cis/trans isomers,[16] we decided to investigate PyTTFs as potential core structures for soluble TTF-based semiconductors. An analogous heteroaromatic-fused TTF, dithieno[3,4-*d*]TTF (DT−TTF), has been previously reported to produce high-performance OFETs having μ_{FET} values as high as 1.4 cm^2 V^{-1} s^{-1}.[13] Here, we report the synthesis and characterization of a series of bis(*N*-alkylpyrrolo)TTFs with long alkyl groups (**3**−**7**), fabrication of OFETs based on their spin-coated thin films, and FET characteristics of the devices.

Experimental Procedures

General. All chemicals and solvents were of reagent grade unless otherwise indicated. DMF was distilled from CaH_2 under reduced pressure. Hexane was distilled from CaH_2 under nitrogen atmosphere. Bis(pyrrolo[3,4-*d*])tetrathiafulvalene (**1**), bis(*N*-methylpyrrolo[3,4-*d*])tetrathiafulvalene (**2**), and bis(*N*-*n*-butylpyrrolo[3,4-*d*])tetrathiafulvalene (**3**) were prepared according to the reported procedure.[16] NMR spectra were obtained in deuterated solvents with a JEOL Lambda 400 spectrometer operating at 400 MHz for ^{1}H and at 100 MHz for ^{13}C with tetramethylsilane as internal reference; chemical shifts (δ) were reported in parts per million. EI-MS spectra were obtained on a Shimadzu QP-5050A spectrometer using an electron impact ionization procedure (70 eV). MALDI-TOF-MS spectra were obtained on a Shimadzu KRATOS KOMPACT MALDI spectrometer. The molecular ion peaks of the sulfur-

(4) (a) Heeney, M.; Bailey, C.; Genevicius, K.; Shkunov, M.; Sparrowe, D.; Tierney, S.; McCulloch, I. *J. Am. Chem. Soc.* **2005**, *127*, 1078−1079. (b) McCulloch, I.; Heeney, M.; Bailey, C.; Genevicius, K.; MacDonald, I.; Shkunov, M.; Sparrowe, D.; Tierney, S.; Wagner, R.; Zhang, W.; Chabinyc, M. L.; Kline, R. J.; McGehee, M. D.; Toney, M. F. *Nat. Mater.* **2006**, *5*, 328−333. (c) McCulloch, I.; Bailey, C.; Giles, M.; Heeney, M.; Love, I.; Shkunov, M.; Sparrowe, D.; Tierney. S. *Chem. Mater.* **2005**, *17*, 1381−1385. (d) Pan, H.; Li, Y.; Wu, Y.; Liu, P.; Ong, B. S.; Zhu, S.; Xu, G. *Chem. Mater.* **2006**, *18*, 3237−3241. (e) Li, Y.; Wu, Y.; Ong, B. S. *Macromolecules* **2006**, *39*, 6521−6527. (f) Li, Y.; Wu, Y.; Liu, P.; Birau, M.; Pan, H.; Ong, B. S. *Adv. Mater.* **2006**, *18*, 3029−3032. (g) Usta, H.; Lu, G.; Facchetti, A.; Marks, T. J. *J. Am. Chem. Soc.* **2006**, *128*, 9034−9035. (h) Crouch, D. J.; Skabara, P. J.; Lohr, J. E.; McDouall, J. J. W.; Heeney, M.; McCulloch, I.; Sparrowe, D.; Shkunov, M.; Coles, S. J.; Horton, P. N.; Hursthouse, M. B. *Chem. Mater.* **2005**, *17*, 6567−6578.

(5) (a) Katz, H. E.; Laquindanum, J. G.; Lovinger, A. J. *Chem. Mater.* **1998**, *10*, 633−638. (b) Murphy, A. R.; Fréchet, J. M. J.; Chang, P.; Lee, J.; Subramanian, V. *J. Am. Chem. Soc.* **2004**, *126*, 1596−1597. (c) Zen, A.; Bilge, A.; Galbrecht, F.; Alle, R.; Meerholz, K.; Grenzer, J.; Neher, D.; Scherf, U.; Farrell, T. *J. Am. Chem. Soc.* **2006**, *128*, 3914−3915. (d) Takimiya, K.; Sakamoto, K.; Otsubo, T.; Kunugi, Y. *Chem. Lett.* **2006**, *35*, 942−943.

(6) (a) Herwig, P. T.; Müllen, K. *Adv. Mater.* **1999**, *11*, 480−483. (b) Afzali, A.; Dimitrakopoulos, C. D.; Breen, T. L. *J. Am. Chem. Soc.* **2002**, *124*, 8812−8813. (c) Weidkamp, K. P.; Afzali, A.; Tromp, R. M.; Hamers, R. J. *J. Am. Chem. Soc.* **2004**, *126*, 12740−12741. (d) Gelinck, G. H.; Huitema, H. E. A.; Van Veenendaal, E.; Cantatore, E.; Schrijnemakers, L.; Van Der Putten, J. B. P. H.; Geuns, T. C. T.; Beenhakkers, M.; Giesbers, J. B.; Huisman, B. H.; Meijer, E. J.; Benito, E. M.; Touwslager, F. J.; Marsman, A. W.; Van Rens, B. J. E.; De Leeuw, D. M. *Nat. Mater.* **2004**, *3*, 106−110.

(7) Laquindanum, J. G.; Katz, H. E.; Lovinger, A. J. *J. Am. Chem. Soc.* **1998**, *120*, 664−672.

(8) Mushrush, M.; Facchetti, A.; Lefenfeld, M.; Katz, H. E.; Marks, T. J. *J. Am. Chem. Soc.* **2003**, *125*, 9414−9423.

(9) (a) Payne, M. M.; Parkin, S. R.; Anthony, J. E.; Kuo, C.-C.; Jackson, T. N. *J. Am. Chem. Soc.* **2005**, *127*, 4986−4987. (b) Dickey, K. C.; Anthony, J. E.; Loo, Y.-L. *Adv. Mater.* **2006**, *18*, 1721−1726.

(10) A recent review on TTF materials: Otsubo, T.; Takimiya, K. *Bull. Chem. Soc. Jpn.* **2004**, *77*, 43−58.

(11) (a) Mas-Torrent, M.; Rovira, C. *J. Mater. Chem.* **2006**, *16*, 433−436. (b) Mas-Torrent, M.; Durkut, M.; Hadley, P.; Ribas, X.; Rovira, C. *J. Am. Chem. Soc.* **2004**, *126*, 984−985. (c) Mas-Torrent, M.; Hadley, P.; Bromley, S. T.; Ribas, X.; Tarrés, J.; Mas, M.; Molins, E.; Veciana, J.; Rovira, C. *J. Am. Chem. Soc.* **2004**, *126*, 8546−8553. (d) Mas-Torrent, M.; Hadley, P.; Bromley, S. T.; Crivillers, N.; Veciana, J.; Rovira, C. *Appl. Phys. Lett.* **2005**, *86*, 12110. (e) Bromley, S. T.; Mas-Torrent, M.; Hadley, P.; Rovira, C. *J. Am. Chem. Soc.* **2004**, *126*, 6544−6545.

(12) (a) Noda, B.; Katsuhara, M.; Aoyagi, I.; Mori, T.; Taguchi, T.; Kambayashi, T.; Ishikawa, K.; Takezoe, H. *Chem. Lett.* **2005**, *34*, 392−393. (b) Katsuhara, M.; Aoyagi, I.; Nakajima, H.; Mori, T.; Kambayashi, T.; Ofuji, M.; Takanishi, Y.; Ishikawa, K.; Takezoe, H.; Hosono, H. *Synth. Met.* **2005**, *149*, 219−223.

(13) (a) Naraso Nishida, J.; Ando, S.; Yamaguchi, J.; Itaka, K.; Koinuma, H.; Tada, H.; Tokito, S.; Yamashita, Y. *J. Am. Chem. Soc.* **2005**, *127*, 10142−10143. (b) Naraso Nishida, J.; Kumaki, D.; Tokito, S.; Yamashita, Y. *J. Am. Chem. Soc.* **2006**, *128*, 9598−9599.

(14) Recently, solution-processed OFETs using zone-casting or spin-coating methods based on tetrakis(alkylthio)-TTF and -bisTTFs were reported: (a) Miskiewicz, P.; Mas-Torrent, M.; Jung, J.; Kotarba, S.; Glowacki, I.; Gomar-Nadal, E.; Amabilino, D. B.; Veciana, J.; Krause, B.; Carbone, D.; Rovira, C.; Ulanski, J. *Chem. Mater.* **2006**, *18*, 4724−4729. (b) Gao, X.; Wu, W.; Liu, Y.; Qiu, W.; Sun, X.; Yu, G.; Zhu, D. *Chem. Commun.* **2006**, 2750−2752.

(15) (a) Simonsen, K. B.; Svenstrup, N.; Lau, J.; Simonsen, O.; Mork, P.; Kristensen, G. J.; Becher, J. *Synthesis* **1996**, 407−418. (b) Takimiya, K.; Aso, Y.; Ogura, F.; Otsubo, T. *Chem. Lett.* **1995**, 735−736. (c) Takimiya, K.; Oharuda, A.; Aso, Y.; Ogura, F.; Otsubo, T. *Chem. Mater.* **2000**, *12*, 2196−2204.

(16) (a) Jeppesen, J. O.; Takimiya, K.; Jensen, F.; Becher, J. *Org. Lett.* **1999**, *1*, 1291−1294. (b) Jeppesen, J. O.; Takimiya, K.; Jensen, F.; Brimert, T.; Nielsen, K.; Thorup, N.; Becher, J. *J. Org. Chem.* **2000**, *65*, 5794−5805.

Table 1. Crystal Data for 3−6

	3	4	5	6
empirical formula	$C_{18}H_{22}N_2S_4$	$C_{26}H_{38}N_2S_4$	$C_{34}H_{54}N_2S_4$	$C_{42}H_{70}N_2S_4$
Fw	394.63	506.84	619.05	731.27
cryst color, habit	yellow, block	yellow, block	yellow, block	yellow, platelet
cryst dimensions (mm^3)	0.50 × 0.20 × 0.10	0.50 × 0.40 × 0.25	0.30 × 0.20 × 0.05	0.30 × 0.25 × 0.20
cryst syst	monoclinic	monoclinic	triclinic	triclinic
lattice params	a = 10.237(4) Å	a = 9.9291(4) Å	a = 4.659(4) Å	a = 5.394(3) Å
	b = 11.170(4) Å	b = 10.8460(5) Å	b = 7.680(8) Å	b = 7.502(3) Å
	c = 8.139(4) Å	c = 12.6025(3) Å	c = 23.82(2) Å	c = 26.92(2) Å
			α = 80.75(3)°	α = 92.34(2)°
	β = 91.51(2)°	β = 92.511(1)°	β = 83.92(3)°	β = 94.06(2)°
			γ = 85.96(3)°	γ = 103.68(2)°
	V = 930.3(7) $Å^3$	V = 1355.88(9) $Å^3$	V = 835(5) $Å^3$	V = 1053.8(9) $Å^3$
space group	$P2_1a$ (No. 14)	$P2_1a$ (No. 14)	$P\bar{1}$ (No. 2)	$P\bar{1}$ (No. 2)
Z value	2	2	1	1
temp (K)	200	200	200	200
no. of reflns measured	total: 9216	total: 12909	total: 8184	total: 7768
	unique: 2134 (R_{int} = 0.053)	unique: 3094 (R_{int} = 0.061)	unique: 3430 (R_{int} = 0.199)	unique: 3938 (R_{int} = 0.045)
no. of reflns (all, 2θ, <55.0°)	1641	2628	1599	2751
no. of variables	109	145	181	217
residuals: R and R_w	0.044 and 0.16	0.034 and 0.102	0.083 and 0.275	0.056 and 0.178
GOF	1.08	1.02	0.8	0.93

containing compounds showed a typical isotopic pattern, and all mass peaks are reported based on ^{32}S. Cyclic voltammograms (CVs) were recorded on a Hokuto Denko HA-301 potentiostat and a Hokuto Denko HB-104 function generator in benzonitrile containing tetrabutylammonium hexafluorophosphate ($TBAPF_6$, 0.1 M) as the supporting electrolyte, at a scan rate of 100 mV/s. Counter and working electrodes were made of Pt, and the reference electrode was Ag/AgCl.

Synthesis of Bis(*N*-alkylpyrrolo[3,4-*d*])tetrathiafulvalenes. Bis(*N*-*n*-octylpyrrolo[3,4-*d*])tetrathiafulvalene (4). Bis(pyrrolo-[3,4-*d*])tetrathiafulvalene (**1**) (434 mg, 1.54 mmol) was dissolved in dry DMF (50 mL), cooled to 0 °C, and deaerated by an argon stream for 15 min. 1-Bromooctane (2.19 g, 15.4 mmol) was added to the mixture, and then sodium hydride (0.485 g, 11.1 mmol) washed with dry hexane was added in one portion. The mixture was stirred for 1.5 h at 0 °C. Brine (200 mL) was added, and the resulting yellow precipitate was collected by filtration, washed with water, and dried in vacuo. The yellow solid was collected and purified by column chromatography (silica gel, CH_2Cl_2) to give **4** as a yellow solid (R_f = 0.7). Recrystallization from hexane gave analytically pure **4** as yellow needles (380 mg, 75%): mp 165.5−166.5 °C; ^1H NMR ($CDCl_3$) δ 0.87 (t, J = 7.0 Hz, 6H), 1.26 (m, 20H), 1.71 (m, 4H), 3.79 (brs, 4H), 6.43 (s, 4H); ^{13}C NMR (DMSO-d_6) δ = 13.9, 22.0, 25.9, 28.5, 30.8, 31.1, 49.8, 113.2, 116.5, 118.9; MS (EI, 70 eV) m/z = 506 (M^+); Anal. calcd for $C_{26}H_{38}N_2S_4$: C, 61.61; H, 7.56; N, 5.53. Found: C, 61.60; H, 7.54; N, 5.54. CV: $E^{ox}_{1/2}$ = +0.33 V, +0.75 V vs Ag/AgCl.

Bis(*N*-*n*-dodecylpyrrolo[3,4-*d*])tetrathiafulvalene (5). The title compound was synthesized in a similar manner to **4** to give yellow needles (hexane) in 61% yield: mp 126.5−127.5 °C; ^1H NMR ($CDCl_3$) δ 0.88 (t, J = 7.0 Hz, 6H), 1.25 (m, 36H), 1.71 (m, 4H), 3.79 (brs, 4H), 6.43 (s, 4H); ^{13}C NMR (C_6D_6) δ 14.4, 23.2, 26.7, 29.5, 29.9 (×2), 30.08, 30.14 (×2), 31.5, 32.4, 50.3, 112.3, 119.3, 120.8; MS (EI, 70 eV) m/z = 618 (M^+); Anal. calcd for $C_{34}H_{54}N_2S_4$: C, 65.96; H, 8.79; N, 4.53. Found: C, 65.94; H, 9.08; N, 4.53. CV: $E^{ox}_{1/2}$ = +0.34 V, +0.75 V.

Bis(*N*-*n*-cetylpyrrolo[3,4-*d*])tetrathiafulvalene (6). A yellow powder from hexane; 79% yield; mp 120.0−121.0 °C; ^1H NMR ($CDCl_3$) δ 0.88 (t, J = 6.8 Hz, 6H), 1.25 (m, 52H), 1.57 (m, 4H), 3.79 (brs, 4H), 6.49 (s, 4H); ^{13}C NMR (C_6D_6) δ 14.4, 23.1, 26.7, 29.5, 29.9 (×2), 30.08, 30.16 (×2), 30.22 (×4), 31.5, 32.4, 50.4, 112.3, 119.4, 120.8; MS (EI, 70 eV) m/z = 730 (M^+); Anal. calcd for $C_{42}H_{70}N_2S_4$: C, 68.98; H, 9.65; N, 3.83. Found: C, 68.97; H, 9.69; N, 3.86. CV: $E^{ox}_{1/2}$ = +0.33 V, +0.75 V.

Scheme 1. Syntheses of Bis(*N*-alkylpyrrolo[3,4-*d*])tetrathiafulvalene Derivatives (2−7) and Their Solubility in Toluene at Room Temperature

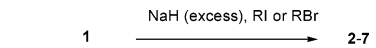

	R	Yield (%)	Solubility (g L^{-1})
2	CH_3	79	<0.01
3	*n*-butyl	71	10
4	*n*-octyl	75	29
5	*n*-dodecyl	61	50
6	*n*-cetyl	79	4.0
7	*n*-icosyl	53	0.4

Bis(*N*-*n*-icosylpyrrolo[3,4-*d*])tetrathiafulvalene (7). A yellow powder from hexane; 53% yield; mp 120.7−121.7 °C; ^1H NMR ($CDCl_3$) δ = 0.88 (t, J = 6.8 Hz, 6H), 1.25 (m, 68H), 1.71 (m, 4H), 3.79 (t, J = 6.8 Hz, 4H), 6.43 (s, 4H);^{13} C NMR (100 MHz, C_6D_6) δ 14.3, 23.1, 26.8, 29.5, 29.82, 29.84, 30.05, 30.13 (×2), 30.21 (×8), 50.4, 112.3, 119.6, 120.9; MS (MALDI-TOF) m/z = 842.51 (M^+); Anal. calcd for $C_{50}H_{86}N_2S_4$: C, 71.20; H, 10.28; N, 3.32. Found: C, 71.06; H, 10.25; N, 3.21. CV: $E^{ox}_{1/2}$ = +0.34 V, +0.76 V vs Ag/AgCl.

Solubility Determination. To a precisely weighed sample (ca. 5 or 10 mg), toluene was added in increments of 0.1 mL, and the resulting mixture was shaken and sonicated at room temperature (20−25 °C). The total amount of toluene required to dissolve the entire solid sample was converted into solubility (g L^{-1}): **3**: 10 g L^{-1}; **4**: 29 g L^{-1}; **5**: 50 g L^{-1}; **6**: 4.0 g L^{-1}; and **7**: 0.4 g L^{-1}.

X-ray Diffraction (XRD) Measurements. XRD measurements of thin films fabricated on the Si/SiO_2 substrate were obtained with a Rigaku RINT 2200 diffractometer with a Cu Kα source (λ = 1.541 Å) in air. Single-crystal X-ray structural analyses were conducted on a Rigaku Rapid-S imaging plate (Mo Kα radiation, λ = 0.71069 Å, graphite monochromator, T = 200 K, and $2\theta_{max}$ = 55.0°). The structure was solved by direct methods.[17] Non-hydrogen atoms were refined anisotropically, and hydrogen atoms were included in the calculations but not refined.[18] All calculations were performed using the crystallographic software package TeXsan 1.19.[19]

(17) SIR-92: Altomare, A.; Cascarano, G.; Giacovazzo, C.; Gugliardi, A.; Burla, M. C.; Polidori, G.; Camalli, M. *J. Appl. Crystallogr.* **1994**, *27*, 435−436.

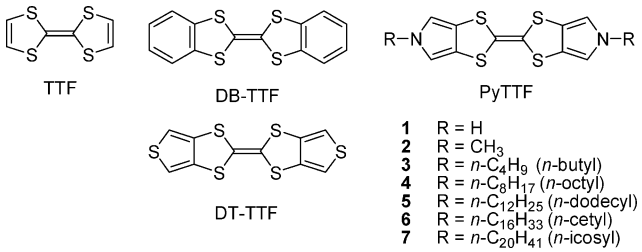

Figure 1. Structures of TTF and its aromatic-fused derivatives, DB-TTF, DT-TTF, and PyTTFs **1**−**7**.

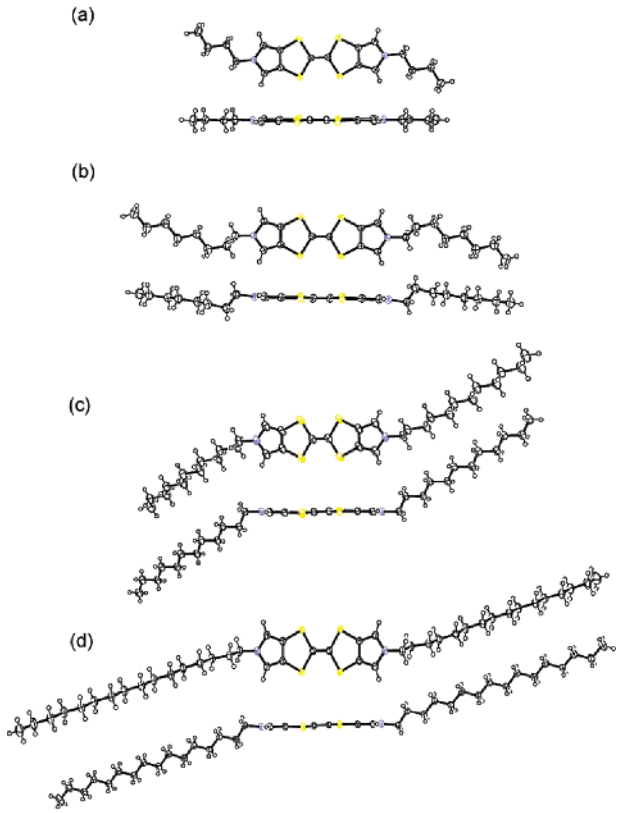

Figure 2. Molecular structures of **3** (a), **4** (b), **5** (c), and **6** (d).

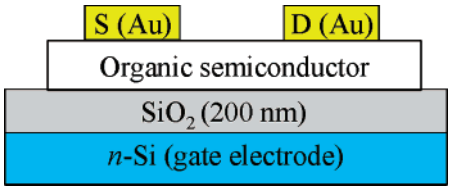

Figure 3. Schematic representation of FET devices.

Fabrication and Evaluation of OFET Devices. Fabrication of OFET devices was carried out in ambient conditions without isolation from ambient oxygen, moisture, or light. Top-contact OFET devices were fabricated on a heavily doped n^+-Si (100) wafer, with a 200 nm thermally grown SiO_2 ($C_i = 17.3$ nF cm^{-2}) dielectric layer. A semiconductor layer was first deposited on the Si/SiO_2 substrate by spin-coating a 0.4 wt % solution of PyTTFs (**3**−**6**) in toluene at 2000 rpm for 30 s and air drying. Because of the relatively low solubility in toluene, the *n*-icosyl derivative (**7**) was dissolved in hot chlorobenzene (80 °C). On top of the organic thin film, gold films (80 nm thick), as the drain and source

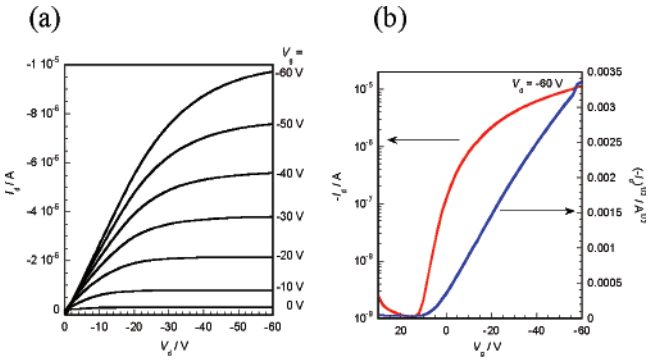

Figure 4. FET characteristics of **7**-based device: (a) output characteristics and (b) transfer characteristics.

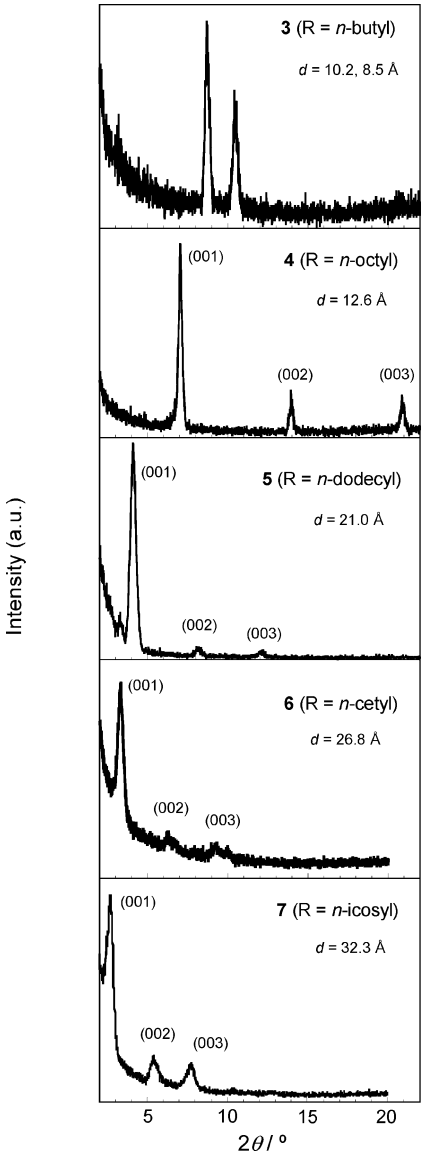

Figure 5. XRD spectra of spin-coated thin films of **3**−**7**.

electrodes, were vacuum-deposited through a shadow mask (back pressure: ∼5 × 10^{-4} Pa). The drain-source channel length (L) and width (W) were 50 μm and ca. 1.5 mm, respectively. Characteristics of the OFET devices were measured at room temperature in air with a Keithley 6430 subfemtoammeter and a Keithley 2400 source meter, operated by a LabTracer program and GPIB interface. μ_{FET} was calculated in the saturation regime of drain current (I_d) using the equation $I_d = (WC_i/2L)\mu_{FET}(V_g - V_{th})$,[2] where C_i is the

(18) Sheldrick, G. M. *Program for the Refinement of Crystal Structures*; University of Göttingen: Göttingen, Germany, 1997.
(19) *teXsan: Single Crystal Structure Analysis Software, Version 1.19*; Molecular Structure Corporation and Rigaku Corporation: 2000.

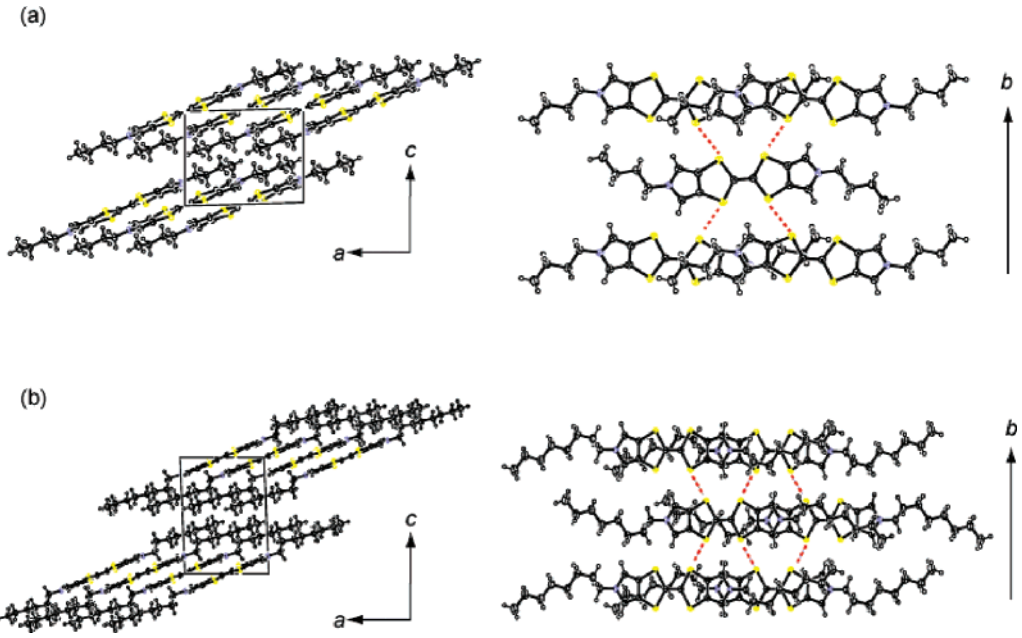

Figure 6. Crystal structures of **3** (a) and **4** (b): side views of molecular layers (*b*-axis projection, left) and projections of one layer normal to the PyTTF plane (right). Side-by-side S−S short distances indicated by dashed lines are 3.63 Å for **3** and 3.36 Å for **4**.

Table 2. FET Characteristics of Bis(pyrrolo)tetrathiafulvalene-Based OFETs[a]

	R	μ_{FET} ($cm^2\ V^{-1}\ s^{-1}$)	I_{on}/I_{off}
2 (10)[b]	CH_3[c]	5.1×10^{-5}	10
3 (4)[b]	*n*-butyl[d]	1.7×10^{-5}	10
4 (16)[b]	*n*-octyl[d]	*e*	
5 (13)[b]	*n*-dodecyl[d]	6.8×10^{-3}	2×10^2
6 (12)[b]	*n*-cetyl[d]	1.3×10^{-2}	10^4
7 (15)[b]	*n*-icosyl[f]	1.3×10^{-2}	10^4

[a] Top-contact configuration with gold source and drain electrodes was used. Channel length (L) and channel width (W) are 50 μm and 1.5 mm, respectively. [b] Numbers in parentheses are the number of devices tested. [c] Evaporated thin film was used as an active layer. [d] 0.4 wt % solution in toluene was used. [e] No reproducible field effect was observed. [f] 0.4 wt % solution in chlorobenzene (ca. 80 °C) was used.

capacitance of the SiO_2 insulator, and V_g and V_{th} are the gate and threshold voltages, respectively.

Results and Discussion

Synthesis and Characterization. A series of bis(*N*-alkylpyrrolo[3,4-*d*])TTFs was synthesized according to the reported procedures (Scheme 1).[16] For comparison with the FET characteristics of evaporated thin-film-based OFETs, a known methyl derivative (**2**) was also synthesized. All alkyl derivatives were isolated as stable yellow powders or crystals and fully characterized by spectroscopic and elemental analyses. To evaluate the solubilizing effect of the introduced alkyl groups, the solubilities of **2**−**7** were determined semiquantitatively (see Experimental Procedures). Although the methyl derivative (**2**) was virtually insoluble, elongation of the alkyl groups enhanced the solubility, as expected. However, in compounds with very long alkyl groups (i.e., **6** with *n*-cetyl groups and **7** with *n*-icosyl groups), the solubility was decreased (Scheme 1). These results indicate that some elongation of the alkyl groups enhances the affinity to solvents by enhancing molecular solubility but that very long alkyl groups, such as the *n*-icosyl group, facilitate strong intermolecular hydrophobic interactions between the groups, consequently reducing the solubility of the molecules.

Table 3. Interlayer Spacing (*d*-Spacing) of Thin Films of 3−7

	R	d (Å)[a]	δ_d (Å)[b]
3	*n*-butyl	8.5, 10.2	
4	*n*-octyl	12.6	4.0
5	*n*-dodecyl	21.0	8.5
6	*n*-cetyl	26.8	5.8
7	*n*-icosyl	32.3	5.5

[a] Determined on the basis of the first-layer line in thin-film XRDs. [b] Increment of *d*-spacing (δ_d) by elongation of alkyl groups with the addition of four CH_2 units; $\delta_d = d_n - d_{n-1}$.

Among the PyTTFs investigated in this study, *n*-butyl (**3**), *n*-octyl (**4**), *n*-dodecyl (**5**), and *n*-cetyl (**6**) derivatives afforded single crystals of high quality that could be fully characterized by single-crystal XRD (Table 1). Figure 2 shows the molecular structures of **3**−**6**, where the PyTTF cores are almost flat in all compounds but the alkyl groups have different conformations. The *n*-butyl groups in **3**, taking an all-anti conformation, lie on the same plane as that of the PyTTF core, whereas the *n*-octyl groups in **4** take a partial gauche conformation, and at the second methylene carbon from the nitrogen atoms in the pyrrole rings, the CH_2 moiety is normal to the PyTTF plane, while the rest of the *n*-octyl groups lie on almost the same plane as that of the PyTTF core. These molecular structures most likely minimize the space required, enabling dense packing in bulk crystals (vide infra). In contrast to the fairly flat molecular structures of **3** and **4**, **5** and **6** form stretched, doubly bent molecular structures in which the *n*-dodecyl groups in **5** and the *n*-cetyl groups in **6** take a staggered, all-anti conformation that minimizes the steric energy in the aliphatic chains.

Deposition of Thin Films by Spin-Coating and Evaluation of FET Devices. As previously mentioned, the present *N*-alkyl-substituted PyTTF derivatives (except **7**) were soluble enough to be spun from various solvents (e.g., dichloromethane, chloroform, THF, toluene, and chlorobenzene). Among these solvents, toluene enabled the reproducible formation of homogeneous thin films of **3**−**6** by spin-coating on the Si/SiO_2 substrate. In contrast, homogeneous

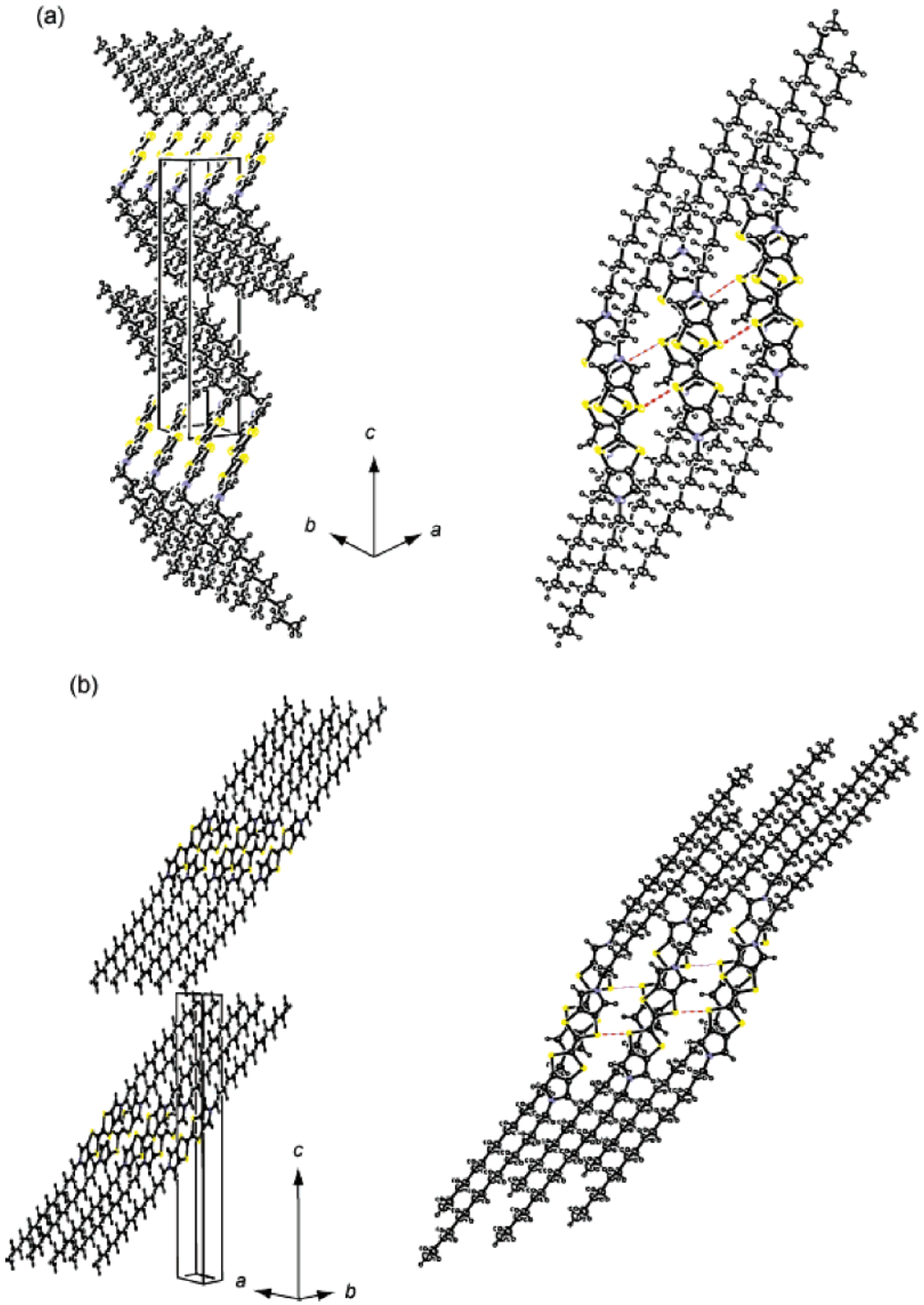

Figure 7. Crystal structures of **5** (a) and **6** (b): side views of molecular layers (left) and projection of one layer normal to the PyTTF plane (right). Side-by-side S−S short distances indicated by dashed lines are 3.43 Å for **5** and 3.40 Å for **6**.

thin films of **7**, which has *n*-icosyl groups and showed a low solubility in toluene at room temperature, were obtained only when a warm solution of **7** in chlorobenzene (ca. 80 °C) was used. Fabrication of top-contact FET devices was completed by vapor deposition of the gold source and drain electrodes through a shadow mask on top of the organic thin films (Figure 3). For comparison, FET devices based on the *N*-methyl derivative (**2**) were also fabricated by a vacuum process.

Evaluation of the devices was carried out under ambient conditions without any precautions taken to eliminate air and moisture. Table 2 summarizes the FET characteristics of the devices evaluated immediately after fabrication.[20] The data were obtained by averaging several devices independently fabricated with each compound. OFETs using evaporated thin films of **2** showed poor FET characteristics with a very small field-effect modulation of drain current; thus, μ_{FET} and I_{on}/I_{off} are very low.[21] Inferior FET characteristics ($\mu_{FET} = \sim 10^{-5}$ cm^2 V^{-1} s^{-1} and $I_{on}/I_{off} = \sim 10$) were also observed

(20) The devices were degraded gradually under ambient conditions, probably owing to the low oxidation potentials (i.e., high HOMO levels) of **3**−**7**. See Supporting Information.

for **3**-based devices fabricated by the spin-coating method. Similarly, most of the **4**-based devices showed no current modulation on gate bias application, and thus, the FET parameters of the devices were not determined (Table 2).

In sharp contrast, **5**-based devices showed a typical *p*-channel FET response with $\mu_{FET} = 6.8 \times 10^{-3}$ cm^2 V^{-1} s^{-1} and $I_{on}/I_{off} = 2 \times 10^2$. Spin-coated thin films of **6** and **7** with long alkyl groups also acted as semiconducting channels in the devices, and the FET mobilities of these devices were in the order of 10^{-2} cm^2 V^{-1} s^{-1} with $I_{on}/I_{off} = 10^4$ (Figure 4 and Table 2). These FET characteristics are fairly good for solution-processible OFET devices and comparable to OFETs based on poly(3-hexylthiophene) tested in our laboratory.[3a,22]

Evaluation of Molecular Ordering by XRD Studies of Thin Films and Bulk Single Crystals. Thin-Film XRD. Figure 5 shows the XRD patterns of thin films of **3**−**7** deposited on an Si/SiO$_2$ substrate by spin-coating. As all the films (except **3)** showed a series of peaks assignable to (00*l*) reflections, it is clear that well-oriented crystalline films were formed. Calculated *d*-spacings based on the first-layer line are listed in Table 3. For the thin film of **3**, there exist two intense peaks at $2\theta = 8.7$ and 10.4°, which correspond to *d*-spacings of 10.2 and 8.5 Å, respectively, indicating the existence of two crystalline phases or two different orientations normal to the substrate surface.

The calculated *d*-spacings were increased with the elongation of the alkyl groups, which may be qualitatively understood by considering that longer molecules form thicker layers. However, focusing on the increment of the *d*-spacing (δ_d) by the addition of four CH$_2$ units, a large increase of *d*-spacing from **4** to **5** is noticeable, which may correspond to a change of molecular orientation. Interestingly, the trend of FET characteristics is also drastically changed at this point, and thus, we speculate that the change of molecular orientation in the thin film and the FET characteristics can be correlated.

To gain further insight into the relationship between molecular orientation and FET characteristics, we examined the structures of **3**−**6** in bulk single crystals. By comparing the *d*-spacings with the cell parameters of the bulk single crystals (Table 1), we noticed a similarity between *d*-spacings and crystallographic *c*-axes in the bulk single crystals, indicating that the preferred orientation normal to the substrate in the thin films is the *c*-axis for all the compounds.

Molecular Orientation in Bulk Single Crystals. Regardless of the length of alkyl groups, the crystal structures of **3**−**6** seemed to be similar to one another, that is, there is a layer-by-layer structure consisting of alternately stacked aliphatic layers and PyTTF layers (Figures 6 and 7). However, detailed examination of the molecular packing revealed that intermolecular interactions, and consequently intermolecular overlaps, are very much dependent on the compounds and dominate the carrier transport properties of FET devices. Interestingly, these four crystal structures can

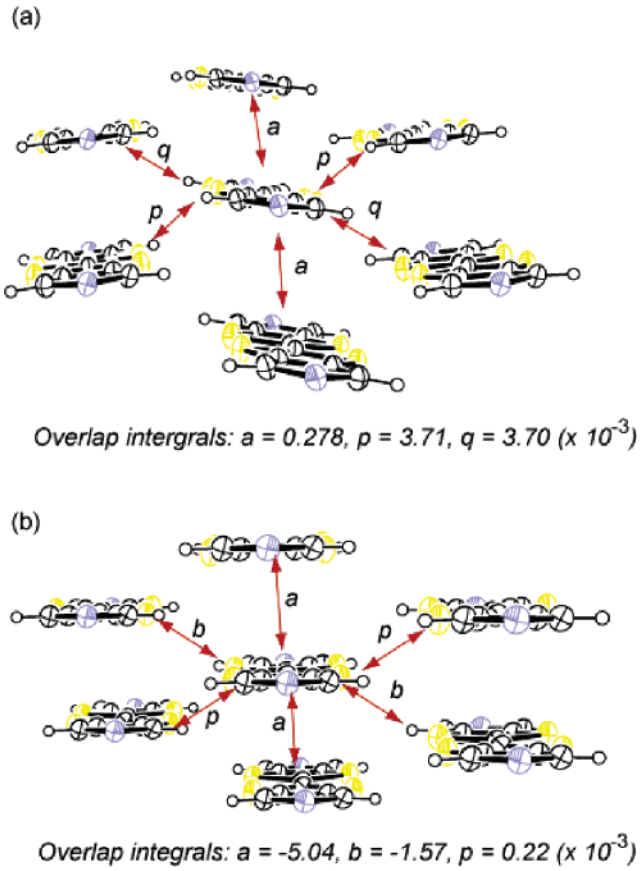

Figure 8. Detailed molecular arrangement in the PyTTF layer for **4** (a) and **6** (b). (For clarity, the alkyl groups of **4** and **6** were omitted.)

be classified into two groups from the viewpoint of molecular arrangement: one is **3** and **4** with a monoclinic space group (Figure 6), and the other is **5** and **6** with a triclinic space group (Figure 7).

In the PyTTF layers of the former two crystal structures with relatively short alkyl groups (**3** and **4**), the molecules tilt markedly from the *c*-axis (Figure 6, left), resulting in the formation of very thin active semiconducting layers where no stacking of the TTF cores exists owing to the slipping of molecules along the long-axis direction (Figure 6, right). Therefore, molecular overlap along the *a*-axis direction is very small, although there are intermolecular side-by-side interactions through S−S contacts in the *b*-axis direction (3.63 Å for **3** and 3.36 Å for **4**).

In contrast, in the PyTTF layers of the latter group (**5** and **6**), both close stacking between PyTTF moieties in the *a*-axis direction and transverse intermolecular interaction through S−S contacts (3.43 Å for **5** and 3.40 Å for **6**) was observed. This indicates that these two compounds have typical two-dimensional (2-D) TTF conducting layers, as observed in many highly conducting charge-transfer TTF salts (Figure 7).[23] The existence of 2-D conducting layers on the substrate is considered to be one of the critical prerequisites to realizing high-performance OFET devices.[24] From these structural features, it appears that the FET characteristics of the present PyTTF-based OFETs are well-

(21) Poor FET characteristics can be ascribed to the less-ordered molecular array in the evaporated thin film of **2**. See Supporting Information.
(22) FET characteristics of P3HT-based devices similarly fabricated are available in the Supporting Information.

(23) (a) Mori, T. *Bull. Chem. Soc. Jpn.* **1998**, *71*, 2509−2526. (b) Mori, T.; Mori, H.; Tanaka, S. *Bull. Chem. Soc. Jpn.* **1999**, *72*, 179−197.

explained by the electronic nature of the semiconducting layer.

To estimate intermolecular overlap more quantitatively, calculation of overlap integrals in the PyTTF layer of each group was carried out using programs developed by Mori et al.[25] As a representative of the former group, the PyTTF layer in the crystal of **4** projected along the molecular long axis is shown in Figure 8a, together with the calculated overlap integrals. The overlap integral along the stacking direction designated as *a* is less than one-tenth of those in the side-by-side directions (designated as *p* and *q*), confirming the lack of 2-D intermolecular interaction in this group of PyTTFs. On the other hand, the calculated overlap integrals of the latter group shown in Figure 8b indicate well the existence of 2-D molecular overlap in the solid state, that is, overlap integrals in the stacking direction (*a*) and in the side-by-side direction (*b*) have the same order of magnitude.

Conclusion

In summary, we have developed a series of *N*-alkyl-substituted PyTTFs (**3**−**7**) as highly soluble TTF derivatives, characterized their solid-state structures by means of XRD studies, and examined them as materials for solution-processible OFET devices. The introduction of long alkyl groups can enhance solubility, whereas very long alkyl groups such as the *n*-icosyl group reduce solubility. This reduced solubility is most likely due to the intermolecular hydrophobic interaction between the very long alkyl groups. The solid-state structure (i.e., molecular packing in the solid state) is also influenced by the length of the alkyl groups. Molecules **5**−**7**, which have *n*-dodecyl or longer alkyl groups, tend to take 2-D molecular ordering both in the bulk single crystals and in the spin-coated thin films, whereas **3** and **4** with relatively short *n*-butyl and *n*-octyl groups are not as susceptible to forming a 2-D interactive structure in the solid state. These results indicate that an appropriate combination of a π-conjugated core with long alkyl groups produces soluble organic semiconductors and that these can form well-organized, 2-D molecular packings in the thin-film state using solution deposition methods.

Consistent with the solid-state structure of the PyTTF derivatives, the FET characteristics of their solution-processed OFETs largely depend on the length of the alkyl groups. Although spin-coated thin films of **3** and **4** were inferior semiconducting layers ($\mu_{FET} = \sim 10^{-5}$ cm^2 V^{-1} s^{-1} or no reproducible field effect), OFET devices consisting of spin-coated thin films of **5**−**7** were capable of affording 2-D solid-state structures, showing typical *p*-channel FET characteristics with hole mobilities of $\sim 10^{-2}$ cm^2 V^{-1} s^{-1} and current on/off ratios of $\sim 10^4$.

The present FET performances are not the best among recently reported high-performance solution-processible OFETs. However, an important conclusion that can be drawn from the present study is that an appropriate combination of a π-conjugated core based on a small molecule with long alkyl groups can provide organic semiconductors capable of affording high-quality thin films with a well-organized 2-D molecular array, which can act as an active semiconducting channel showing a field-effect mobility of $\sim 10^{-2}$ cm^2 V^{-1} s^{-1}.

Acknowledgment. This work was partially supported by a Grant-in-Aid for Scientific Research from the Ministry of Education, Culture, Sports, Science and Technology, Japan and an Industrial Technology Research Grant Program in 2006 from the New Energy and Industrial Technology Development Organization (NEDO), Japan.

Supporting Information Available: CIF for **3**−**6**, electrochemical data and UV−vis spectra of **2**−**7**, detailed evaluation of device characteristics, device fabrication by vapor deposition of **2**, XRD of thin films of **2**, and FET characteristics of **2**-based devices. Characteristics of P3HT-based devices fabricated and evaluated using the same experimental methods as those for **3**−**7**. This material is available free of charge via the Internet at http://pubs.acs.org.

CM070956+

(24) (a) Cornil, J.; Calbert, J.-P.; Beljonne, D.; Silbey, R.; Brédas, J.-L. *Adv. Mater*. **2000**, *12*, 978−983. (b) Cornil, J.; Calbert, J.-P.; Brédas, J.-L. *J. Am. Chem. Soc*. **2001**, *123*, 1250−1251. (c) Cornil, J.; Beljonne, D.; Calbert, J.-P.; Brédas, J.-L. *Adv. Mater*. **2001**, *13*, 1053−1067.

(25) Mori, T.; Kobayashi, A.; Sakai, Y.; Kobayashi, H.; Saito, G.; Inokuchi, H. *Bull. Chem. Soc. Jpn*. **1984**, *57*, 627−633.